HHS Public Access

Author manuscript

ACS Chem Biol. Author manuscript; available in PMC 2024 April 21.

Published in final edited form as:

ACS Chem Biol. 2023 April 21; 18(4): 693–700. doi:10.1021/acschembio.1c00840.

Effects of Oncohistone Mutations and PTM Crosstalk on the N-terminal Acetylation Activities of NatD

Yi-Hsun Ho,

Rong Huang*

Department of Medicinal Chemistry and Molecular Pharmacology, Purdue Institute for Drug Discovery, Purdue University Center for Cancer Research, Purdue University, West Lafayette, Indiana 47907, United States

Abstract

Acetylation at the α-N-terminus (Nα) is the most abundant modification detected on histone H4 and H2A, which is catalyzed by N-terminal acetyltransferase D (NatD or NAA40). Histone H4 and H2A contain an identical N-terminal SGRGK sequence that is enriched with post-translational modifications (PTMs) and frequently occurred oncogenic mutations known as “oncohistone” mutations. However, there is a lack of information on how oncohistone mutations and other PTMs affect NatD-catalyzed acetylation. Herein, we determined how the local chemical environment on the N-terminal SGRGK sequence regulates NatD-catalyzed Nα-acetylation on histone H4/H2A. Our studies indicate that all oncohistone mutations at SGRG suppressed the acetylation catalyzed by NatD. Meanwhile, H4 Ser1 phosphorylation and Arg3 methylation negatively impact the NatD-mediated acetylation, but the Lys5 acetylation only has a marginal effect. This work reveals the impacts of oncohistone mutations on NatD activity and unravels the crosstalk between NatD and PTMs, implying potential regulatory mechanism of NatD and highlighting different avenues to interrogate the NatD-mediated pathway in the future.

Graphical Abstract

***Corresponding Author:** Rong Huang, Department of Medicinal Chemistry and Molecular Pharmacology, Purdue Institute for Drug Discovery, Purdue University Center for Cancer Research, Purdue University, West Lafayette, Indiana 47907, United States. huang-r@purdue.edu.

Author Contributions

The manuscript was written through the contributions of both authors. Both authors have approved the final version of the manuscript.

Supporting Information.

The following files are available free of charge.

Kinetic profiles, MALDI-MS, and HPLC spectra of all peptides.

The authors declare no competing financial interest.

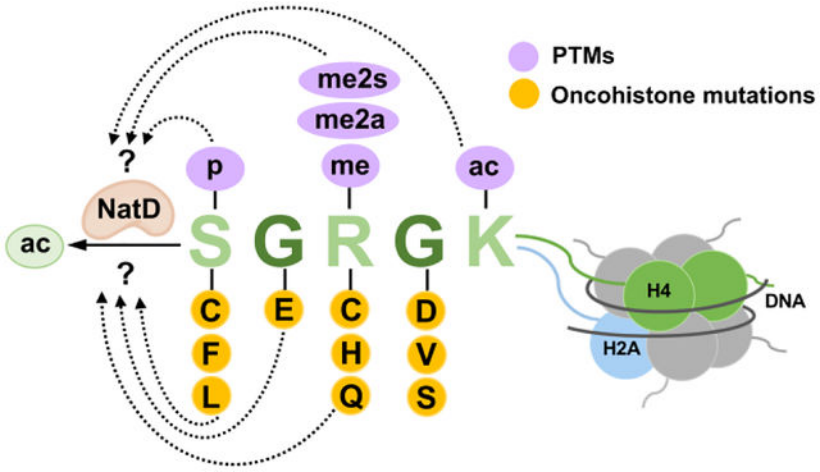

Keywords

Acetylation; NatD; Oncohistones; Acetyltransferase; Arginine methylation

Introduction.

Histone modifications alter the chromatin structures and DNA accessibility, serving as a critical mechanism in the regulation of gene expression, DNA replication, and DNA repair.[1,2] Concerning the modification type and site, over 450 modifications have been identified on histones, such as phosphorylation, methylation, and acetylation.[3] Crosstalk among these modifications adds another dimension to the dynamical regulation of transcription.[2] The α-N-terminal (Nα) acetylation is a dominant modification for approximately 80% of proteins in humans.[4–6] This modification is catalyzed by N-terminal acetyltransferases (NATs), which have been classified into NatA–H based on their subunit compositions and substrate specificity profiles.[5] Among NATs, NatD (also known as NAA40, Nat4, or Patt1) contains only one catalytic unit, NAA40, which specifically acetylates an SGRG sequence at the protein N-terminus (Figure 1A). Until now, H4 and H2A are the only two confirmed protein substrates for NatD.[7–10] Notably, Nα-acetylation of H4 (Nα-acH4) and H2A (Nα-acH2A) were the most abundant marks of histone proteins through quite a few proteomic investigations.[11–16] For instance, over 80% of H4 and H2A were found Nα-acetylated in mouse brains;[14] and 97–98% of Nα-acH4 was reported in breast cancer cell lines.[11]

Several recurrent mutations including H3K27M, H3G34R, H3K36M, and H2B-E76K have been identified as epigenetic drivers of several cancers.[17–19] Thus, these histone mutants are termed “oncohistone” mutations.[20] Besides these four established oncohistone mutations, the newly identified mutational landscape for all four core histones across different tumor types has expanded the scope of oncohistones, although the underlying mechanisms of most mutants remain uncharacterized.[20] Interestingly, multiple mutations have been identified in the SGRG recognition motif of NatD (Figure 1B).[20–23] Notably, Ser1 and Arg3 are the top two frequently mutated residues of H4; and Ser1 is the most frequently mutated residue of

H2A.[20] Nevertheless, the knowledge of how those newly discovered H4/H2A mutations spur cancer is limited by the lack of understanding of how these mutations affect biological and biochemical processes that converge on chromatin remodeling and accessibility. Therefore, as a starting point, we undertake to investigate how oncohistone mutations at the N-terminal regions affect NatD-catalyzed Nα-acetylation.

Meanwhile, the H4 tail is abundant with post-translational modifications (PTMs), including phosphorylation, methylation, and acetylation. Nα-acH4 has been found to affect other PTMs at Ser1, Arg3, and Lys5 on H4 to influence biological outcomes.[24–29] For instance, Nα-acH4 interfered with asymmetrical dimethylation on H4 Arg3 residue (H4R3me2a) in yeast.[24,25] Caloric restriction in yeast suppressed NatD expression and increased the ratio of H4R3me2a to Nα-acH4, promoting the expression of metabolic and stress-response genes.[25] Consistent with the findings in yeast, a biochemical study demonstrated that Nα-acetylation on H4 peptide reduced the rate of H4R3me2a catalyzed by protein arginine methyltransferase 1 (PRMT1) and PRMT3 but had a marginal effect on the Arg3 dimethylation by PRMT5 and PRMT8.[27,29] In colorectal cancer, loss of Nα-acH4 decreased symmetric dimethylation on H4 Arg3 (H4R3me2s) levels by downregulating PRMT5, but has a trivial effect on monomethylation (H4R3me1) or H4R3me2a.[28] Nα-acH4 has been demonstrated to block casein kinase 2α-mediated phosphorylation at the Ser1 (H4pS1) in lung cancer cells, inducing Slug expression and metastasis.[26] Additionally, knockdown of NatD increased H4pS1 and H4R3me2a but slightly reduced H4R3me2s while H4K5ac remained unchanged based on western analysis. However, both H4K5ac and H4R3me2a were decreased on the Slug promoter in NatD knockdown cells according to ChIP analysis.[26] Although Nα-acetylation on H4 influenced Arg3 methylation, Ser1 phosphorylation, and Lys5 acetylation, it remains elusive if the communication is unidirectional or mutual. Because the first four residues SGRG are critical for substrate recognition, we hypothesize that modifications on and adjacent to SGRG may affect NatD-catalyzed Nα-acetylation. Herein, we also set out to examine how the post-translational modifications of H4S1, H4R3, and H4K5 affect Nα-acetylation by NatD (Figure 1B).

RESULTS AND DISCUSSION.

Effect of histone H4/H2A length on NatD activity.

Previous studies suggested that yeast NatD requires a more extended substrate peptide sequence for Nα-acetylation than human NatD (hNatD).[7] Specifically, complete acetylation was detected in yeast when the first 50 residues of H4 were present but incomplete in the presence of the first 30 residues.[7] In contrast, hNatD displayed a comparable catalytic efficiency for H4 synthetic peptides consisting of the first 5, 8, and 19 residues in a biochemical radioactive study.[10] To systematically understand how substrate length affects hNatD catalysis, we determined the steady-state kinetic parameters for both full-length H4 protein and a panel of truncated H4/H2A synthetic peptides using recombinant hNatD and a continuous fluorescence assay.[30] The steady-state parameters are comparable for H4 protein and the cofactor acetyl coenzyme A (AcCoA) (Figure 2A). While hNatD exhibited comparable k_{cat} values for its substrates with variable lengths ranging from full-length protein to a tripeptide (Figure 2B), the k_{cat}/K_m values of hNatD varied for different lengths

of substrates (Figure 2C), indicating that the substrate length affects the substrate binding by NatD. But once substrates bind to the enzyme and form the substrate-enzyme complex (ES), no major difference in the turnover number of NatD as k_{cat} values are similar.

Notably, hNatD demonstrated equivalent activity and efficiency for both H4-21 and full-length H4 protein, suggesting that the following sequence after Val21 does not contribute to hNatD recognition. When peptide length decreased from H4-21 to H4-12, no changes were observed for the catalytic activity of hNatD bound with substrate molecules as reflected by k_{cat} values (11 ± 0.37 min^{-1}, 11 ± 0.35 min^{-1}, and 10 ± 0.26 min^{-1}, respectively). However, there was about a 2.5-fold decrease in the k_{cat}/K_m values for H4-12. A similar trend was observed when the peptide length was reduced from 12 to 8 residues. When the peptide length decreased from 5 to 4 and 4 to 3 residues, the k_{cat}/K_m values decreased about 5-fold and 8-fold, respectively, which suggested the significant contribution of the last five residues to the association by hNatD. Similar fold changes were observed for H2A peptides when reduced from 21 to 12 and 12 to 8 residues, respectively. The first five residues SGRGK are the same for both H4 and H2A at their N-termini, but three longer H2A peptides (H2A-21, H2A-12, and H2A-8) exhibited an about 4-fold reduction in k_{cat}/K_m values compared to corresponding H4 peptides, inferring a modest preference of hNatD for H4 over H2A. In addition, we also synthesized a pentapeptide SGRGA derived from a predicted protein substrate SMARCD2, an SWI/SNF-related chromatin regulator.[31] Compared to H4-5 (also H2A-5), SGRGA demonstrated a similar k_{cat} and k_{cat}/K_m values within less than 2-fold difference. In summary, the k_{cat} values were comparable for peptide substrates with varying lengths from 3–21 residues, while the k_{cat}/K_m values of nine investigated peptide substrates were inversely proportional to their length (Figure 2B, C). This result agrees with the previous study on the crucial contribution from the first four N-terminal residues to NatD-specific binding.[9,10] Nevertheless, the backbone interaction of the fifth residue also plays a contributing role to the interaction.

Nα-acetylation of Oncohistone H4 and H2A.

The H4 and H2A are the only two validated substrates of hNatD, containing an identical SGRGK motif at their N-termini. The high-frequency mutations observed in the first four residues of H4/H2A prompted us to investigate how Nα- acetylation is affected by H4/H2A oncohistone mutations.[20] Hence, we synthesized pentapeptides derived from the N-terminus of oncohistones H4/H2A and determined their steady-state kinetic parameters using a continuous fluorescence assay (Figure 3A). Since the fluorescence assay monitors the acetylation progression through detecting the thiol group in the CoA,[30] the cysteine residue in pentapeptides that carry S1C or R3C mutation would interfere with the assay. Therefore, we utilized a previously developed MALDI-MS assay to directly detect acetylated products for the peptides with S1C and R3C mutation (Figure S1).[32] Because cysteine is prone to oxidize, a reducing agent dithiothreitol (DTT) was added to the reaction mixture to prevent dimer formation. For 1 mM of cysteine-containing peptides, 5 mM DTT was selected to completely suppress the dimer formation. To compare the performance of two assays and the effect of DTT, we used H4-5 as control and performed kinetic analysis for H4-5 using the MALDI-MS assay in the presence or absence of 5 mM DTT (Figure S1A, B). The steady-state kinetic parameters obtained from the MALDI-MS assay are comparable to

those from the fluorescence assay, validating the feasibility of comparing results from two different assays for the Cys-containing peptides.

Ser1 and Gly2 are two critical residues for substrate-binding with hNatD because the small hydroxyl side chain of Ser1 and a specific angle of Gly2 enable the substrate to enter into the substrate-binding pocket of hNatD.[10] In H4 and H2A, S1C is one of the high-frequency mutations detected in bladder, colorectal, lung, and liver cancers.[20] As shown in Figure 3A, hNatD displayed an approximate k_{cat} of 7 min^{-1} and ~100-fold reduction in k_{cat}/K_m value for S1C mutant that only replaces the hydroxyl side chain of Ser1 with a thiol group. We also employed the MALDI-MS assay to determine the kinetics of S1F because of unknown interference from S1F with the fluorescence assay (Figure S1). When the bulky phenylalanine (F) is at the first position, hNatD exhibited a k_{cat} of 6.8 min^{-1} and over 1,000-fold decrease in k_{cat}/K_m value. Mutations of Ser1 with Cys or Phe resulted in a significant reduction in the substrate association with hNatD while marginally affecting the turnover number. Compared to H4-5, the k_{cat} values of S1L and G2E mutations were decreased 5- and 3-fold, respectively (Figure 3B, Figure S2). Furthermore, S1L and G2E mutations caused a dramatic reduction in k_{cat}/K_m values by over 10,000-fold (2.5×10^2 and 1.4×10^2 $M^{-1}min^{-1}$, respectively), suggesting that S1L and G2E mutations affect both substrate-enzyme interaction to form ES and the turnover number (Figure 3C).

Arg3 contributes to the binding of the substrate by hNatD through several interactions with the side chains of Asp127, Glu129, Tyr136, and Tyr138 of hNatD.[10] R3H mutant of H2A has been observed in uterine and ovarian carcinomas.[21] In comparison to H4-5, the k_{cat} values were decreased by 3-fold to 3.7 ± 0.12 min^{-1} for R3Q and 1.5-fold to 7.5 ± 0.13 min^{-1} for R3H (Figure 3B). Interestingly, the R3H mutant displayed a moderate change in k_{cat}/K_m by 6.5-fold (2.9×10^5 M^{-1} min^{-1}). Conversely, a 200-fold reduction in k_{cat}/K_m (9.4×10^3 $M^{-1}min^{-1}$) was observed in the R3Q mutant. Similarly, hNatD displayed a 17-fold reduction in k_{cat}/K_m for the R3C mutant (1.1×10^5 $M^{-1}min^{-1}$). This difference in k_{cat}/K_m between R3Q, R3H, and R3C is consistent with the hNatD mutagenesis study that demonstrated the importance of the positive charge at the third residue for substrate binding.[10]

Like Gly2, Gly4 resides in a narrow groove that is tailored for glycine. Mutation of Gly4 to aspartic acid (G4D) or valine (G4V) resulted in slightly decreased k_{cat} values by less than 2-fold (8.0 ± 0.66 and 7.7 ± 0.13 min^{-1}, respectively). Despite the similar k_{cat} values, hNatD displayed a 7-fold higher k_{cat}/K_m for G4V (2.1×10^5 M^{-1} min^{-1}) than G4D (2.9×10^4 M^{-1} min^{-1}), suggesting G4D less favorable to ES formation than G4V. When Gly4 was mutated to serine (G4S), hNatD exhibited a 17- and 7-fold reduction in k_{cat}/K_m and k_{cat} values, respectively. The co-crystal structure of hNatD in complex with its substrate peptide (PDB: 4U9W) indicated that Gly4 interacts with Trp90, Thr174, and Tyr211.[10] However, it is unclear why G4S resulted in a salient reduction in k_{cat} value among three mutations at the Gly4 residue.

Crosstalk between other PTMs and Nα-acetylation.

Several PTMs have been demonstrated to be affected by Nα-acetylation at the H4 to induce different gene expression patterns.[24,26,28] Knockdown of NatD increased H4pS1 and

H4R3me2a but slightly reduced H4R3me2s in lung cancer H1299 cells according to western blot analysis.[26] However, reduction of Nα-acH4 led to decreased H4R3me2a and H4K5ac but increased H4pS1 on the Slug promoter through ChIP analysis.[26] On the other hand, Nα-acH4 transcriptionally induces PRMT5 expression and thus increases the H4R3me2s in colorectal cancer cells.[28] To determine how chemical modifications with charges and steric properties on the substrate peptides affect hNatD activity, we thus synthesized and determined the steady-state kinetics of several H4 peptides carrying common PTMs (Figure 4A). hNatD showed a 2.3-fold drop in k_{cat} (4.6 ± 0.090 min^{-1}) and over 100-fold reduction in k_{cat}/K_m to acetylate H4pS1 peptide (Figure 4B, C). As hNatD has a restrictive size pocket that favors a small side chain, phosphorylation on Ser1 may not be tolerable in the pocket. In addition, the negatively charged phosphate group may also clash with the Glu139 of hNatD.[10] Thus, it is not surprising that phosphorylation at Ser1 negatively impacts Nα-acetylation.

The guanidino group of the Arg3 side chain interacts with Asp127, Glu129, and Tyr138 of NatD through hydrogen bonds.[10] Our biochemical studies showed that hNatD had a similar k_{cat} value for methylated H4R3 peptides despite different methylation states (me1, me2a, or me2s) compared to unmodified H4-5 (Figure 4B, Figure S2). However, the impacts of methylation states on k_{cat}/K_m are different. Specifically, hNatD displayed 3.6-fold decreased k_{cat}/K_m for H4R3me1 (5.2×10^5 M^{-1} min^{-1}), while 8- and 17-fold reduction in k_{cat}/K_m were observed for H4R3me2a and H4R3me2s, respectively (Figure 4C). As previous biochemical studies reported that Nα-acetylation of H4 slightly reduced PRMT1, 3, 5, and 8 activity on Arg3 dimethylation, our findings suggest the effects between Nα-acetylation and Arg3 dimethylation are mutually inhibitory.[27,29] On the occasion of Lys5 acetylation (H4K5ac), hNatD exhibited comparable kinetic parameters for H4K5ac as H4-5. One possible explanation is that the side chain of Lys5 has less contribution to NatD substrate-binding because of its exposure to solvent,[10] which is also supported by the result that SGRGA peptide displays comparable parameters as SGRGK peptide (Figure 2).

Inhibitory activities of mutant and modified H4 against NatD.

Although the oncogenic roles of oncohistone remain underexplored, recent studies found that the oncohistone mutation affected the chromatin remodeling processes and thus resulted in oncogenic gene dysregulation and carcinogenesis.[19,33] Another profound effect of oncohistone mutations is to inhibit the activities of chromatin-modulating enzymes.[34] For example, H3K27M mutant represses H3K27 methylation through inhibition of the enzymatic activity of enhancer of zeste homolog 2 (EZH2), a catalytic component of the polycomb repressive complex 2 (PRC2).[34] In addition, H3K27M also spreads H3K27me2/3 to cause tumorigenesis.[34] To determine the effects of oncohistone mutations and modified H4 peptides on NatD-mediated acetylation, we performed a competitive inhibition assay in the presence of varying concentrations of competitors while H4-5 and AcCoA were kept at their respective K_m concentrations. Among all tested peptides, G4S mutant exerted the strongest inhibition on NatD-mediated acetylation, displaying ~80% inhibition on hNatD even at 33 μM (Figure 5). Since R3C has similar kinetic profiles with G4S, we anticipated R3C might also have similar inhibitory activity with G4S, which will need further investigation. Meanwhile, H4R3me2s demonstrated over 50% inhibition against

NatD-mediated acetylation at 100 μM, exhibiting the highest inhibitory effect among all peptides carrying PTMs (Figure 5).

Conclusion.

In this study, we examined how the length, oncohistone mutations, and PTMs at the substrate recognition motif affect Nα-acetylation catalyzed by hNatD. Based on our results, the oncohistone mutations at Ser1 and Gly2 of H4 and H2A strongly decreased catalytic efficiency of Nα-acetylation by hNatD and hampers substrate recognition by over 100-fold (Figure 6A). Compared with mutations at Ser1 and Gly2, hNatD was moderately inhibited by mutations at Arg3 but only slightly affected by the R3H mutant, which supports the importance of the positive charge status at Arg3. Meanwhile, our studies provide evidence of the negative impacts of phosphorylation of Ser1 and methylation of Arg3 on Nα-acetylation, uncovering the crosstalk between Nα- acetylation and other PTMs. Specifically, phosphorylation of H4S1 suppresses Nα-acetylation by over 100-fold while dimethylation of H4R3 leads to a 10–20 fold decrease in the turnover number of NatD activity. Meanwhile, G4S and H4R3me2s demonstrated the strongest inhibition on NatD-catalyzed acetylation (Figure 6B). As PRMT5 is responsible for producing H4R3me2s and NatD has been shown to regulate PRMT5 expression, it would be interesting to elucidate the mechanisms of interplay between PRMT5 and NatD. In addition to the oncohistone mutations, multiple mutations in NatD were detected in cancer diseases according to a database of somatic mutations in human cancer.[35] Among them, more than 20 mutations occur in the NatD active site, but it is unknown how these mutations affect NatD activity to impact cancer development. Meanwhile, crosstalk between Nα-acetylation and PTMs poses a challenging question if NatD introduces Nα-acetylation co-translationally or post-translationally or both. Here, the proposed model based on our biochemical studies establishes a relationship between Nα-acetylation and local PTMs of histones and oncohistones, outlining the basis for future investigation on the functions of the NatD-mediated pathway.

METHODS.

General.

The standard Fmoc-protected amino acids were purchased from CEM Corporation. Acetyl coenzyme A lithium salt was purchased from Sigma-Aldrich. ThioGlo4 was purchased from Berry & Associates. High-performance liquid chromatography (HPLC) grade solvents were purchased from Fisher Scientific. Matrix-assisted laser desorption/ionization (MALDI) spectra were acquired using positive-ion mode on a 4800 MALDI TOF/TOF mass spectrometry (Sciex). Peptides were synthesized on a CEM Liberty Blue peptide synthesizer. The purity of the peptides was confirmed by Agilent 1260 Series HPLC system, eluting with a 0–40% acetonitrile/water gradient with 0.1% (v/v) TFA. All the purity of final peptides showed >95%. The spectra of MALDI and HPLC are available in the Supporting information (Figure S3).

Peptide Synthesis.

The peptides were synthesized using Rink Amide MBHA resin (0.05 mmol) and followed a standard Fmoc protocol. Fmoc protected amino acids were coupled at 0.2 M in DMF using 0.5 M of DIC and 1.0 M of Oxyma. Double coupling of Fmoc-Ser(HPO_3Bzl)-OH (ChemPep), Fmoc-Arg(me)(Pbf)-OH (AnaSpec), Fmoc-Arg$(me)_2$-OH (asymmetrical and symmetrical) (AnaSpec), Fmoc-Lys(ac)-OH (Creosalus) were performed. Fmoc deprotection was carried out by 20% piperidine in DMF. The resin was washed with CH_2Cl_2 (5 mL) and MeOH (5 mL) alternatively three times, and the peptide was cleaved by a cleavage cocktail (TFA/TIPS/water/DODT = 94/1/2.5/2.5 v/v) (5 mL) for 0.05 mmol scale of resin for 4 h. The peptide suspension was filtered, and the filtrate was dried under N_2 and precipitated with cold ether (10 mL). The peptide precipitation was pelleted by centrifugation at 4,200 rpm for 10 minutes, and the resulting supernatant was discarded. The crude peptide pellet was dissolved in deionized water (10 mL), passed through a 0.45 μm filter, and purified by preparative reversed-phase high-performance liquid chromatography (RP-HPLC) on an Agilent 1260 Series system with a C18 column (5 μm, 10 mm × 250 mm) at a flow rate of 4.0 mL/min. Peptides were purified by two mobile phases consisting of 0.1% (v/v) TFA in water and acetonitrile in a linear gradient.

Protein Expression and Purification.

Expression and purification of hNatD were carried out as previously described.[30] Histone H4 protein was a gift from Dr. Chongli Yuan from Purdue University.

Continuous Fluorescence-Based Acetylation Assay.

A fluorescence assay was adapted to study the kinetics of hNatD, which monitors the formation of a ThioGlo4-thiol adduct that exhibits a strong fluorescence at 465 nm.[36,37] hNatD activity was measured at 25 °C under the following conditions in a final reaction volume of 40 μL: 50 nM hNatD, 15 μM ThioGlo4, and 50 μM AcCoA in reaction buffer (25 mM HEPES, 150 mM NaCl, 0.01% (v/v) Triton, pH 7.5). For AcCoA characterization, H4-8 was fixed at 50 μM. All components except for peptide substrate were mixed in a volume of 36 μL and incubated at 25 °C for 10 min. The reaction was initiated by adding 4 μL of varying concentrations of peptide substrates. Fluorescence was monitored on a BMG CLARIOstar microplate reader with excitation of 400–415 nm and 460–485 nm. For quantifying the fluorescent signal, a previously reported standard curve ($y = 5176x + 344.6$) was applied to convert arbitrary fluorescence units to the concentration of CoA.[30] GraphPad Prism 7 was used to fit the initial velocity to Michaelis-Menten or Substrate inhibition model. The experiments were performed in at least duplicate (Figure S2).

MALDI-MS Acetylation Assay.

Acetylation of CGRGK and SGCGK were characterized with a MALDI-MS assay at 25 °C under the following conditions in a final reaction volume of 40 μL: 50 nM of hNatD and 50 μM of AcCoA in reaction buffer (25 mM HEPES, 150 mM NaCl, pH 7.5). The 10 mM cysteine peptides (CGRGK and SGCGK) were allowed to reduce under 50 mM of DTT at room temperature for 30 min. The peptides were then 2-fold diluted from 1 mM (CGRGK) and 400 μM (SGCGK) with dilution buffer (25 mM HEPES, 150 mM NaCl, 10

mM DTT, pH 7.5). All components except for peptide substrate were mixed in a volume of 36 μL, and the reaction was initiated with 4 μL of varying concentrations of peptide substrates. At desired time points, aliquots were quenched in a 1:1 ratio with the 0.1% (v/v) of TFA aqueous solution and spotted with matrix solution (10 mg ml^{-1} of CHCA in water/acetonitrile/TFA = 1:1:0.1% v/v/v) on the MALDI plate. The initial velocity was determined by calculating the slope from aliquots taken at differing time points. GraphPad Prism 7 was used to fit the initial velocity to Michaelis-Menten or Substrate inhibition model. The experiments were performed in duplicate.

Inhibition Assay.

The competitive inhibition study was performed using a previously described fluorescence assay.[38] hNatD activity was measured at 25 °C under the following conditions in a final reaction volume of 40 μL: 50 nM hNatD, 15 μM ThioGlo4, 0.6 μM AcCoA, and 6 μM H4-5 in reaction buffer (25 mM HEPES, 150 mM NaCl, 0.01% (v/v) Triton, pH 7.5). The 10X concentration of mutant or modified peptides was diluted with reaction buffer and then 3-fold serially diluted with reaction buffer. All components (50 nM hNatD, 15 μM ThioGlo4, and 6 μM H4-5) except for AcCoA were mixed in a volume of 32 μL. To the reaction mixture was added 4 μL of the 10X mutant or modified peptides, and the resulting mixture was incubated at room temperature for 10 min. The reaction was then initiated by adding 4 μL of 6 μM AcCoA. Fluorescence was monitored on a BMG CLARIOstar microplate reader with excitation of 400–415 nm and 460–485 nm for 10 min. The control group was the reaction mixture without adding mutant or modified peptides. The reaction rate was obtained by calculating the linear range of the slope generated from fluorescence signals. The hNatD activity was calculated by normalizing the rate of the testing group to that of the control group. The experiments were performed in duplicate.

Supplementary Material

Refer to Web version on PubMed Central for supplementary material.

ACKNOWLEDGMENT

The authors acknowledge C. Park for his critical comments. We are grateful to Y. Zhao for his assistance with several peptide syntheses and C. Yuan for H4 protein.

Funding Sources

We thank the support from the National Institutes of Health R01CA258887 (RH), Department of Medicinal Chemistry and Molecular Pharmacology (RH), and Borch Graduate Endowment Award (YH).

ABBREVIATIONS

NATs
N-terminal acetyltransferase

AcCoA
acetyl-coenzyme A

SMARCD2

SWI/SNF-related matrix-associated actin-dependent regulator of chromatin subfamily D member 2

H4pS1
histone H4 serine 1 phosphorylation

H4R3me2a
H4R3me1, histone arginine 3 monomethylation

histone H4 arginine 3 asymmetric dimethylation

H4R3me2a
histone H4 arginine 3 symmetric dimethylation

H4K5ac
histone H4 lysine 5 acetylation

EZH2
enhancer of zeste homolog 2

PRC2
polycomb repressive complex 2

REFERENCES

(1). Jenuwein T; Allis CD Translating the Histone Code. Science. 2001, 293, 1074–1080. [PubMed: 11498575]

(2). Lee JS; Smith E; Shilatifard A The Language of Histone Crosstalk. Cell 2010, 142, 682–685. [PubMed: 20813257]

(3). Huang H; Sabari BR; Garcia BA; Allis CD; Zhao Y SnapShot: Histone Modifications. Cell 2014, 159, 458–458. [PubMed: 25303536]

(4). Aksnes H; Drazic A; Marie M; Arnesen T First Things First: Vital Protein Marks by N-Terminal Acetyltransferases. Trends Biochem. Sci 2016, 41, 746–760. [PubMed: 27498224]

(5). Aksnes H; Ree R; Arnesen T Co-Translational, Post-Translational, and Non-Catalytic Roles of N-Terminal Acetyltransferases. Mol. Cell 2019, 73, 1097–1114. [PubMed: 30878283]

(6). Demetriadou C; Koufaris C; Kirmizis A Histone N-Alpha Terminal Modifications: Genome Regulation at the Tip of the Tail. Epigenetics and Chromatin 2020, 13, 1–13. [PubMed: 31918747]

(7). Polevoda B; Hoskins J; Sherman F Properties of Nat4, an Nα-Acetyltransferase of *Saccharomyces Cerevisiae* that Modifies N Termini of Histones H2A and H4. Mol. Cell. Biol 2009, 29, 2913–2924. [PubMed: 19332560]

(8). Song O; Wang X; Waterborg JH; Sternglanz R An Nα-Acetyltransferase Responsible for Acetylation of the N-Terminal Residues of Histones H4 and H2A. J. Biol. Chem 2003, 278, 38109–38113. [PubMed: 12915400]

(9). Hole K; Van Damme P; Dalva M; Aksnes H; Glomnes N; Varhaug JE; Lillehaug JR; Gevaert K; Arnesen T The Human N-Alpha-Acetyltransferase 40 (hNaa40p/hNatD) is Conserved from Yeast and N-Terminally Acetylates Histones H2A and H4. PLoS One 2011, 6, e24713. [PubMed: 21935442]

(10). Magin RS; Liszczak GP; Marmorstein R The Molecular Basis for Histone H4- and H2A-Specific Amino-Terminal Acetylation by NatD. Structure 2015, 23, 332–341. [PubMed: 25619998]

(11). Wang T; Holt MV; Young NL Early Butyrate Induced Acetylation of Histone H4 is Proteoform Specific and Linked to Methylation State. Epigenetics 2018, 13, 519–535. [PubMed: 29940793]

(12). Phanstiel D; Brumbaugh J; Berggren WT; Conard K; Feng X; Levenstein ME; McAlister GC; Thomson JA; Coon JJ Mass Spectrometry Identifies and Quantifies 74 Unique Histone H4 Isoforms in Differentiating Human Embryonic Stem Cells. Proc. Natl. Acad. Sci 2008, 105, 4093–4098. [PubMed: 18326628]

(13). Pesavento JJ; Bullock CR; LeDuc RD; Mizzen CA; Kelleher NL Combinatorial Modification of Human Histone H4 Quantitated by Two-Dimensional Liquid Chromatography Coupled with Top Down Mass Spectrometry. J. Biol. Chem 2008, 283, 14927–14937. [PubMed: 18381279]

(14). Tweedie-Cullen RY; Brunner AM; Grossmann J; Mohanna S; Sichau D; Nanni P; Panse C; Mansuy IM Identification of Combinatorial Patterns of Post-Translational Modifications on Individual Histones in the Mouse Brain. PLoS One 2012, 7, e36980. [PubMed: 22693562]

(15). Yamamoto K; Chikaoka Y; Hayashi G; Sakamoto R; Yamamoto R; Sugiyama A; Kodama T; Okamoto A; Kawamura T Middle-Down and Chemical Proteomic Approaches to Reveal Histone H4 Modification Dynamics in Cell Cycle. Mass Spectrom. 2015, 4, A0039.

(16). Jiang T; Hoover ME; Holt MV; Freitas MA; Marshall AG; Young NL Middle-Down Characterization of the Cell Cycle Dependence of Histone H4 Posttranslational Modifications and Proteoforms. Proteomics 2018, 18, 1–11.

(17). Bender S; Tang Y; Lindroth AM; Hovestadt V; Jones DTW; Kool M; Zapatka M; Northcott PA; Sturm D; Wang W; et al. Reduced H3K27me3 and DNA Hypomethylation are Major Drivers of Gene Expression in K27M Mutant Pediatric High-Grade Gliomas. Cancer Cell 2013, 24, 660–672. [PubMed: 24183680]

(18). Lu C; Jain SU; Hoelper D; Bechet D; Molden RC; Ran L; Murphy D; Venneti S; Hameed M; Pawel BR; et al. Cancer: Histone H3K36 Mutations Promote Sarcomagenesis through Altered Histone Methylation Landscape. Science. 2016, 352, 844–849. [PubMed: 27174990]

(19). Bennett RL; Bele A; Small EC; Will CM; Nabet B; Oyer JA; Huang X; Ghosh RP; Grzybowski AT; Yu T; et al. A Mutation in Histone H2B Represents a New Class of Oncogenic Driver. Cancer Discov. 2019, 9, 1438–1451. [PubMed: 31337617]

(20). Nacev BA; Feng L; Bagert JD; Lemiesz AE; Gao J; Soshnev AA; Kundra R; Schultz N; Muir TW; Allis CD The Expanding Landscape of “oncohistone” Mutations in Human Cancers. Nature 2019, 567, 473–478. [PubMed: 30894748]

(21). Zhao S; Bellone S; Lopez S; Thakral D; Schwab C; English DP; Black J; Cocco E; Choi J; Zammataro L; et al. Mutational Landscape of Uterine and Ovarian Carcinosarcomas Implicates Histone Genes in Epithelial–Mesenchymal Transition. Proc. Natl. Acad. Sci 2016, 113, 12238–12243. [PubMed: 27791010]

(22). Koufaris C; Kirmizis A N-Terminal Acetyltransferases Are Cancer-Essential Genes Prevalently Upregulated in Tumours. Cancers (Basel). 2020, 12, 2631. [PubMed: 32942614]

(23). Chew GL; Bleakley M; Bradley RK; Malik HS; Henikoff S; Molaro A; Sarthy J Short H2A Histone Variants Are Expressed in Cancer. Nat. Commun 2021, 12, 1–9. [PubMed: 33397941]

(24). Schiza V; Molina-Serrano D; Kyriakou D; Hadjiantoniou A; Kirmizis A N-Alpha-Terminal Acetylation of Histone H4 Regulates Arginine Methylation and Ribosomal DNA Silencing. PLoS Genet. 2013, 9, e1003805. [PubMed: 24068969]

(25). Molina-serrano D; Schiza V; Demosthenous C; Stavrou E; Oppelt J; Kyriakou D; Liu W; Zisser G; Bergler H; Dang W; et al. Loss of Nat4 and its Associated Histone H4 N-Terminal Acetylation Mediates Calorie Restriction-Induced Longevity. EMBO Rep. 2016, 17, 1829–1843. [PubMed: 27799288]

(26). Ju J; Chen A; Deng Y; Liu M; Wang Y; Wang Y; Nie M; Wang C; Ding H; Yao B; et al. NatD Promotes Lung Cancer Progression by Preventing Histone H4 Serine Phosphorylation to Activate Slug Expression. Nat. Commun 2017, 8, 928. [PubMed: 29030587]

(27). Fulton MD; Zhang J; He M; Ho M-C; Zheng YG Intricate Effects of α-Amino and Lysine Modifications on Arginine Methylation of the N-Terminal Tail of Histone H4. Biochemistry 2017, 56, 3539–3548. [PubMed: 28644004]

(28). Demetriadou C; Pavlou D; Mpekris F; Achilleos C; Stylianopoulos T; Zaravinos A; Papageorgis P; Kirmizis A NAA40 Contributes to Colorectal Cancer Growth by Controlling PRMT5 Expression. Cell Death Dis. 2019, 10, 236. [PubMed: 30858358]

(29). Fulton MD; Dang T; Brown T; Zheng YG Effects of Substrate Modifications on the Arginine Dimethylation Activities of PRMT1 and PRMT5. Epigenetics 2020, 1–18.

(30). Ho Y-H; Chen L; Huang R Development of A Continuous Fluorescence-Based Assay for N-Terminal Acetyltransferase D. Int. J. Mol. Sci 2021, 22, 594. [PubMed: 33435607]

(31). Ring HZ; Vameghi-Meyers V; Wang W; Crabtree GR; Francke U Five SWI/SNF-Related, Matrix-Associated, Actin-Dependent Regulator of Chromatin (SMARC) Genes Are Dispersed in the Human Genome. Genomics 1998, 51, 140–143. [PubMed: 9693044]

(32). Richardson SL; Hanjra P; Zhang G; Mackie BD; Peterson DL; Huang R A Direct, Ratiometric, and Quantitative MALDI–MS Assay for Protein Methyltransferases and Acetyltransferases. Anal. Biochem 2015, 478, 59–64. [PubMed: 25778392]

(33). Bagert JD; Mitchener MM; Patriotis AL; Dul BE; Wojcik F; Nacev BA; Feng L; Allis CD; Muir TW Oncohistone Mutations Enhance Chromatin Remodeling and Alter Cell Fates. Nat. Chem. Biol 2021, 17, 403–411. [PubMed: 33649601]

(34). Harutyunyan AS; Krug B; Chen H; Papillon-Cavanagh S; Zeinieh M; De Jay N; Deshmukh S; Chen CCL; Belle J; Mikael LG; et al. H3K27M Induces Defective Chromatin Spread of PRC2-Mediated Repressive H3K27me2/Me3 and is Essential for Glioma Tumorigenesis. Nat. Commun 2019, 10, 1262. [PubMed: 30890717]

(35). Tate JG; Bamford S; Jubb HC; Sondka Z; Beare DM; Bindal N; Boutselakis H; Cole CG; Creatore C; Dawson E; et al. COSMIC: The Catalogue of Somatic Mutations in Cancer. Nucleic Acids Res. 2019, 47, D941–D947. [PubMed: 30371878]

(36). Richardson SL; Mao Y; Zhang G; Hanjra P; Peterson DL; Huang R Kinetic Mechanism of Protein N-Terminal Methyltransferase 1. J. Biol. Chem 2015, 290, 11601–11610. [PubMed: 25771539]

(37). Dong G; Yasgar A; Peterson DL; Zakharov A; Talley D; Cheng KC-C; Jadhav A; Simeonov A; Huang R Optimization of High-Throughput Methyltransferase Assays for the Discovery of Small Molecule Inhibitors. ACS Comb. Sci 2020, 22, 422–432. [PubMed: 32525297]

(38). Deng Y; Deng S; Ho Y-H; Gardner SM; Huang Z; Marmorstein R; Huang R Novel Bisubstrate Inhibitors for Protein N-Terminal Acetyltransferase D. J. Med. Chem 2021, 64, 8271.

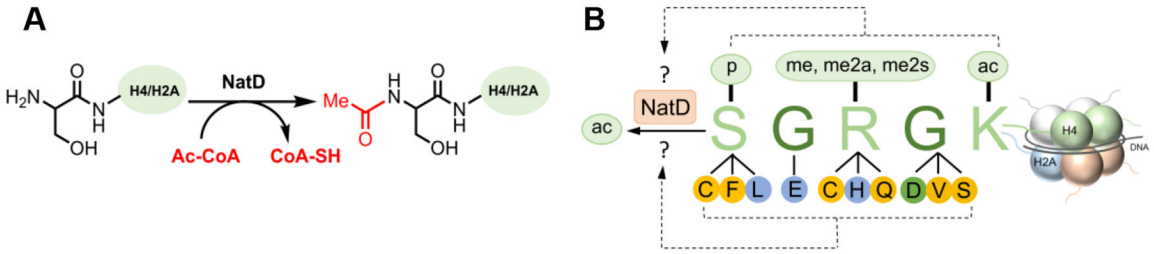

Figure 1.

(A) Nα-acetylation catalyzed by NatD. (B) Mutations of oncohistone H4 and H2A and chemical modifications at residues Ser1, Arg3, and Lys5 on the H4 substrate. Modifications include phosphorylation (p), monomethylation (me), asymmetric dimethylation (me2a), symmetric dimethylation (me2s), and acetylation (ac). Mutations detected on H4 and H2A: yellow circle; mutations detected only on H4: green circle; mutations detected only on H2A: blue circle.

A

ID	Sequence	K_m (μM)	k_{cat} (min^{-1})	k_{cat}/K_m (M^{-1} min^{-1})
Full length histone H4		0.80 ± 0.10	12 ± 0.42	1.5×10^7
H4-21	SGRGKGGKGLGKGGAKRHRKV	0.83 ± 0.095	11 ± 0.37	1.3×10^7
H4-12	SGRGKGGKGLGK	2.1 ± 0.22	11 ± 0.35	5.2×10^6
H4-8	SGRGKGGK	3.8 ± 0.38	10 ± 0.26	2.6×10^6
H4-5	SGRGK	5.9 ± 0.59	11 ± 0.46	1.9×10^6
H4-4	SGRG	28 ± 2.4	11 ± 0.39	3.9×10^5
H4-3	SGR	211 ± 21	9.5 ± 0.48	4.5×10^4
AcCoA	AcCoA	0.63 ± 0.055	9.5 ± 0.48	1.5×10^7
H2A-21	SGRGKQGGKARAKAKTRSSRA	3.5 ± 0.52	11 ± 0.46	3.1×10^6
H2A-12	SGRGKQGGKARA	7.3 ± 0.76	9.2 ± 0.27	1.3×10^6
H2A-8	SGRGKQGG	13 ± 1.2	7.5 ± 0.23	5.8×10^5
SMARCD2-5	SGRGA	9.7 ± 0.45	11 ± 0.17	1.1×10^6

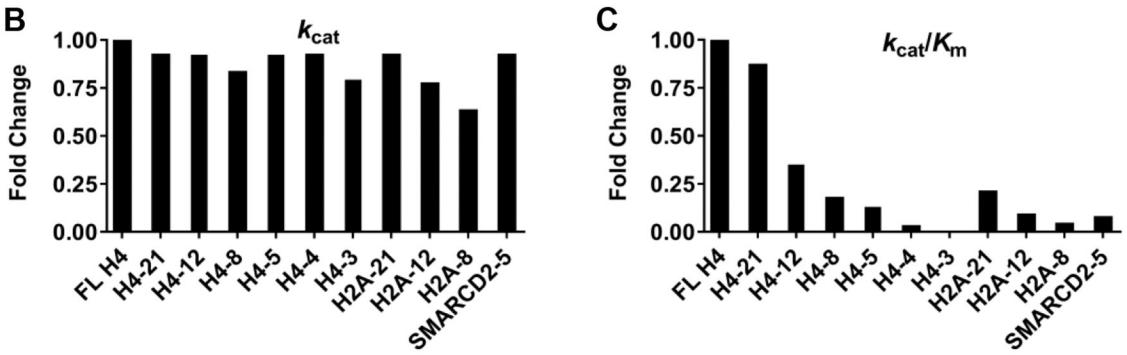

Figure 2.

Effect of C-terminal truncations of hNatD-catalyzed acetylation. (A) Steady-state parameters of AcCoA, C-terminal truncated H4, H2A, and SMARCD2 peptides. Fold changes of (B) k_{cat} and (C) k_{cat}/K_m normalized to full-length histone H4 (FL H4).

A

ID	Mutation count H4	Mutation count H2A	Sequence	K_m (μM)	k_{cat} (min^{-1})	k_{cat}/K_m (M^{-1} min^{-1})
H4-5			SGRGK	5.9 ± 0.59	11 ± 0.46	1.9×10^6
H4/H2A S1C	5	6	CGRGK	> 500	> 7	
H4/H2A S1F	2	2	FGRGK	> 5 mM	> 6.8	
H2A S1L	0	4	LGRGK	8.8 ± 1.9 mM	2.2 ± 0.29	2.5×10^2
H2A G2E	0	3	SERGK	23 ± 2.8 mM	3.3 ± 0.31	1.4×10^2
H4/H2A R3Q	1	1	SGQGK	393 ± 35	3.7 ± 0.12	9.4×10^3
H2A R3H	0	5	SGHGK	26 ± 1.4	7.5 ± 0.13	2.9×10^5
H4/H2A R3C	9	7	SGCGK	17	1.8	1.1×10^5
H4 G4D	4	1	SGRDK	272 ± 40	8.0 ± 0.66	2.9×10^4
H4/H2A G4V	1	4	SGRVK	37 ± 1.6	7.7 ± 0.13	2.1×10^5
H4/H2A G4S	4	3	SGRSK	14 ± 3.1	1.6 ± 0.16	1.1×10^5

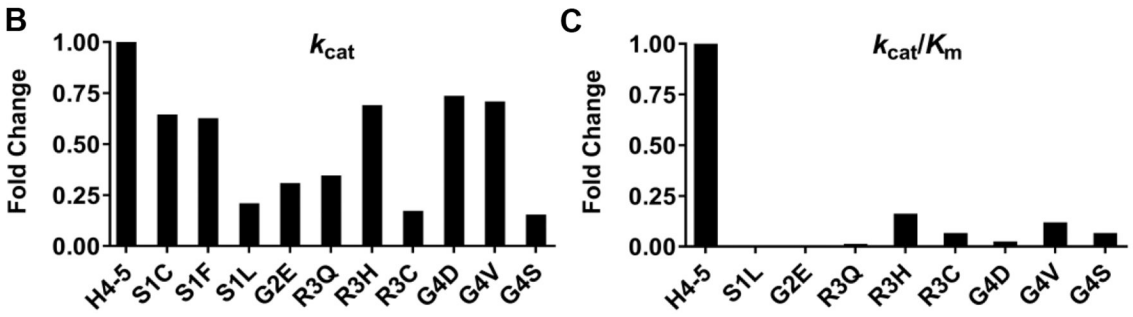

Figure 3.

Effects of oncohistone mutations on N-terminal acetylation of H4/H2A peptides. (A) Kinetic profiles of oncohistone H4/H2A pentapeptides. The mutation count of H4 and H2A was extracted from a processed cBioPortal dataset.[20] Fold change of (B) k_{cat} and (C) k_{cat}/K_m normalized to wild-type H4-5.

A

ID	Sequence	K_m (μM)	k_{cat} (min^{-1})	k_{cat}/K_m (M^{-1} min^{-1})
H4-5	SGRGK	5.9 ± 0.59	11 ± 0.46	1.9×10^6
H4pS1	(p)SGRGK	303 ± 21	4.6 ± 0.090	1.5×10^4
H4R3me1	SGR(me)GK	18 ± 0.91	9.3 ± 0.13	5.2×10^5
H4R3me2a	SGR(me2a)GK	47 ± 3.6	11 ± 0.23	2.3×10^5
H4R3me2s	SGR(me2s)GK	73 ± 12	7.8 ± 0.71	1.1×10^5
H4K5ac	SGRGK(ac)	6.1 ± 0.54	10 ± 0.25	1.6×10^6

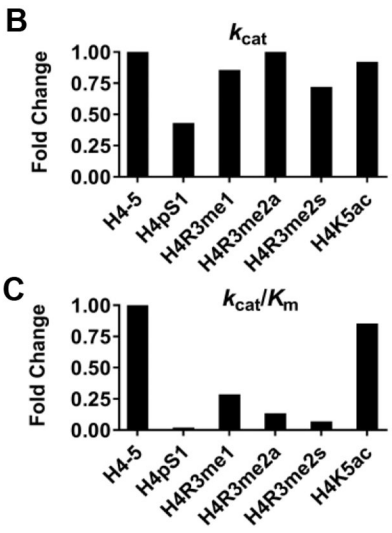

Figure 4.

Effects of PTMs on H4-5 peptide (SGRGK) histone on Nα-acetylation. (A) Steady-state parameters of chemically modified H4 pentapeptides. Fold changes of (B) k_{cat} and (C) k_{cat}/K_m normalized to wild-type H4-5.

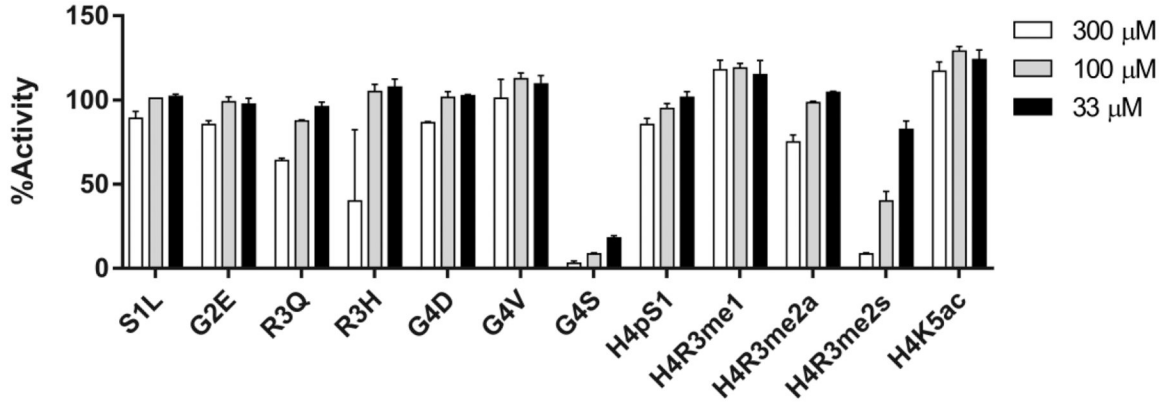

Figure 5.

Inhibitory effects of H4/H2A peptides carrying either oncohistone mutation or PTM on Nα-acetylation by hNatD. The competitive inhibition assay was conducted with a 3-fold serial dilution of mutant and modified peptides starting from 300 μM in the presence of 6 μM of H4-5 and 0.6 μM of AcCoA. The activity was normalized to the activity in the absence of competing peptides.

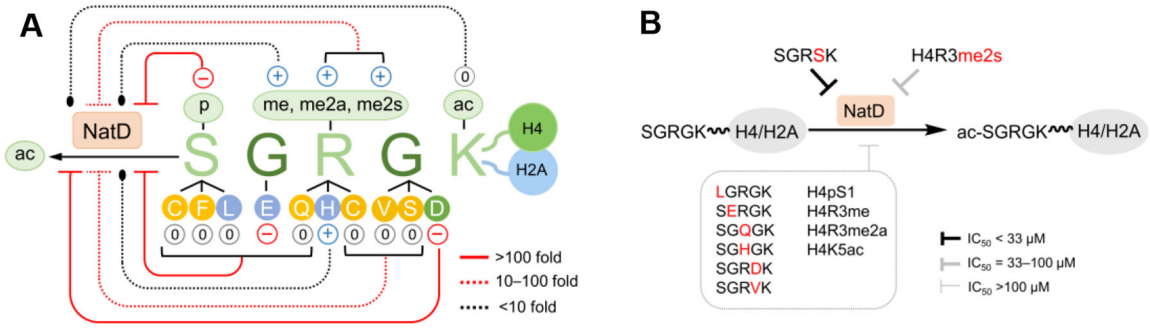

Figure 6.

Impacts of H4/H2A peptides carrying oncohistone mutations or PTMs on NatD-catalyzed acetylation. (A) NatD-catalyzed acetylation on various peptides. PTMs include phosphorylation (p), monomethylation (me), asymmetric dimethylation (me2a), symmetric dimethylation (me2s), and acetylation (ac). Mutations were detected on H4 and H2A (yellow), only on H4 (green), only on H2A (blue). The charge status contains neutral (0 within in a gray circle), positive (+ within in a blue circle), and negative (– within in a red circle). Solid red line with blunt end = over 100-fold decrease, red dotted line with blunt end =10–100-fold decrease, and black dotted line = less than 10-fold decrease. (B) Inhibitory effects on NatD-catalyzed acetylation of H4-5 (SGRGK) in a competitive inhibition assay.